IJST, Transactions of Mechanical Engineering, Vol. 38, No. M1+, pp 195-206
Printed in The Islamic Republic of Iran, 2014

EFFECT OF SLIP VELOCITY AND BEARING DEFORMATION ON THE PERFORMANCE OF A MAGNETIC FLUID BASED ROUGH POROUS TRUNCATED CONICAL PLATES*

M. E. SHIMPI[1**] AND G. M. DEHERI[2]

[1]Birla Vishvakarma Mahavidyalaya Eng. College, Vallabh Vidyanagar, Anand, Gujarat (India)
Email: mukesh.shimpi@gmail.com
[2]Dept. of Mathematics, Sardar Patel University, Vallabh Vidyanagar, Anand, Gujarat (India)

Abstract– An attempt has been made to discuss the behaviour of a magnetic fluid based squeeze film between rough porous truncated conical plates by taking into consideration the effects of bearing deformation and slip velocity. Taking recourse to a different type of probability density function, the model of Christensen and Tonder has been adopted to evaluate the effect of transverse surface roughness and the concern stochastically averaged Reynolds' type equation has been solved to derive the expression for pressure distribution. This results in the calculation of load carrying capacity. The graphical representations make it clear that although the combined effect of bearing deformation and slip velocity is relatively adverse the magnetic fluid lubricant saves the situation to a limited extent, at least in the case of the negatively skewed roughness. For an overall improvement of performance of bearing system, the slip parameter should be minimized. A suitable combination of aspect ratio and semi vertical angle may lead to some compensation for negative effect of deformation, especially when variance (negative) is involved.

Keywords– Truncated conical plates, roughness, magnetic fluid, deformation, slip velocity

1. INTRODUCTION

Prakash and Vij [1] analyzed the squeeze films between porous plates of various shapes such as circular, annular, elliptic, rectangular and conical. In this investigation a comparison was made between the squeeze film performances of various geometries of equivalent surface area with other parameters remaining the same and it was concluded that the circular plates had the highest transient load carrying capacity.

The use of magnetic fluid as a lubricant modifying the performance of a bearing system has been explored and employed in a number of investigations [Verma [2]; Bhat and Deheri [3-4]]. This investigation established that the load carrying capacity increased with increasing magnetization. The squeeze film performance in circular disks had significantly improved as compared to that of the annular plates.

Hsiu at el [5] studied the combined effect of couple stresses and roughness. The transverse roughness caused the reduction in the attitude angle and friction parameters while the effect of longitudinal roughness remained almost opposite to that of transverse roughness.

Deheri et al [6] extended the analysis of Bhat and Deheri [4] to study the effect of surface roughness on the performance of a magnetic fluid based squeeze film between rough porous truncated conical plates. In this investigation Christensen and Tonder [7-9] stochastic model was adopted to evaluate the effect of

*Received by the editors June 22, 2013; Accepted January 1, 2014.
**Corresponding author

transverse surface roughness. This investigation of Deheri et al [6] suggested that there was some scope for minimizing the adverse effect of roughness by the magnetization at least in the case of negative skewed roughness.

Gupta and Deheri [10] analyzed the effect of transverse surface roughness on the performance of a squeeze film in spherical bearing. It was found that among the three roughness parameters the skewness affected the system most and positively skewed roughness caused savoir load reduction.

Andharia et al [11] discussed the effect of transverse surface roughness on the performance of a hydrodynamic slider bearing adopting the stochastic model and found that a transverse roughness resulted in an adverse effect in general. However, the situation remained comparatively better when variance (negative) was involved and this positive effect was aided by the negative skewed roughness.

Hsu at el [12] investigated the combined effect of surface roughness and rotating inertia on the squeeze film performance characteristics of parallel circular disks. It was shown that the surface roughness turned in an adverse effect in general. The rotating inertia further aggravated the situation when relatively higher values of standard deviation were involved.

Schwarz [13] presented a new method to calculate the elastic deformation of a sphere on a flat surface considering the influence of short range and long range attraction forces inside and outside the actual contact area.

Shimpi and Deheri [14-15] extended and developed the analysis of Bhat and Deheri [3-4] respectively by considering the effect of surface roughness and deformation on the behaviour of a magnetic fluid based squeeze film in rotating curved porous circular plates. Here it was established that the deformation effect needed to be minimized to compensate the adverse effect of the porosity and standard deviation by the positive effect of magnetization. The negatively skewed roughness registered relatively more compensation.

Shimpi and Deheri [16] made an effort to study the surface roughness effect on the squeeze film performance between a fluid circular plate under the presence of magnetic fluid. It was noticed that the positive effect of magnetization got a further boost in the presence of negatively skewed roughness.

Shah and Patel [17] discussed the slider bearing of various geometrical shapes incorporating the effects of anisotropic permeability and slip velocity. Mirea and Voicu [18] studied the load bearing capacity of the truncated cone and hemispherical foundations realized in punched holes by resorting to Finite Element Method. The results emphasized a better behaviour for the hemispherical element as compared to the truncated conical element.

Ahmed and Mahdy [19] embarked on a non-similarity analysis for investigating the laminar free convection boundary layer flow over a permeable isothermal truncated cone in the presence of a transverse magnetic field effect. Further, various models of nano-fluid based on different formulae for thermal conductivity and dynamic viscosity on the flow and heat transfer characteristic were discussed.

Nassab et al [20] numerically analyzed lubricant compressibility effect on hydrodynamic characteristics of heavily loaded journal bearings. The result showed that the compressibility effect caused an increase in the generated hydrodynamic pressure.

Rahmatabadi and Rashidi [21] presented the study of the effect of the mount angle on the theoretical static and dynamic characteristics of three types of gas lubricated non circular journal bearings. It was found that the effect of mount angle was more significant at low compressibility number. Nassab and Moayeri [22] dealt with the two dimensional thermo-hydrodynamic analysis of journal bearing characteristics. Numerical solution of full Navier -Stokes equations coupled with energy equation in the lubricant field and heat conduction equation in the bearing were obtained for an infinitely long bearing. Here, we have tried to analyze the effect of bearing deformation, surface roughness and slip velocity on the performance of a magnetic fluid based squeeze film in truncated conical plates taking a different type

of distribution for modeling the surface roughness. This type of bearing system may be used to dilute polymer solutions and in heart valve implants etc.

2. ANALYSIS

The bearing system consists of two truncated conical plates. The upper plate moves towards the lower plate. The bearing surfaces are transversely rough and the porous facing is backed by solid facing. The geometry and coordinates are depicted in the following Figure. For a detailed discussion refer to Prakash and Vij [1].

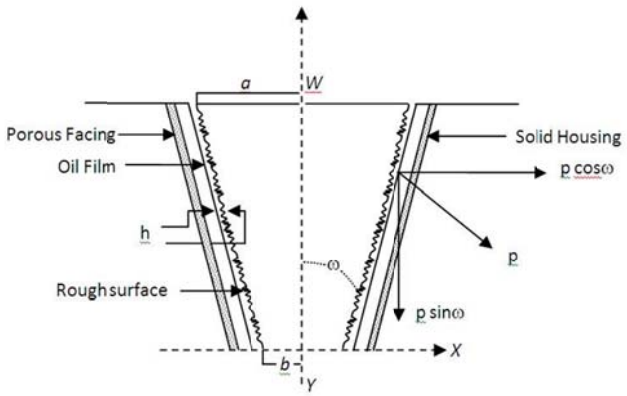

Fig. 1. Configuration of truncated conical plates

Following Tzeng and Saibel [23], the one dimensional film thickness is considered to be of the form

$$h = \bar{h} + h_s, \tag{1}$$

where $\bar{h}$ is the smooth film thickness and h_s constitute the stochastic variation from the smooth film thickness $\bar{h}$. h_s is regarded as a random variable whose probability density function is a beta-distribution given by [Prajapati [24]]

$$f(h_s) = \begin{cases} \frac{15}{16c}\left(1-\frac{h_s^2}{c^2}\right)^2, & -c \le h_s \le c \\ 0, & \textit{elsewhere} \end{cases} \tag{2}$$

The details regarding standard deviation σ, mean α and skewness ε can be had from Christensen and Tonder [7-9]. Here the method of Christensen and Tonder [7-9] has been adopted for stochastically averaging the associated Reynolds' equation.

It is considered that the flow of magnetic fluid between the truncated conical plates is axially symmetric while the magnitude as of the oblique magnetic field $\overline{H}$ is a function of x vanishing at $a\cos ec\omega$ and $b\cos ec\omega$. For example,

$$H^2 = K(acoec\omega - x)(x - bcoec\omega), \quad b < x < a \tag{3}$$

where K is suitably chosen so as to have a magnetic field of required strength, which suits the dimensions of both the sides. The inclination angle of magnetic field with the lower plate is determined as in Deheri et al [6].

Following stochastically averaging the modified Reynolds' type equation governing the film pressure p turns out to be [Prajapati [24]]

$$\frac{1}{x}\frac{d}{dx}\left[x\frac{d}{dx}\left(p - 0.5\mu_0\bar{\mu}H^2\right)\right] = \frac{12\mu\dot{h}\sin\omega}{g(h)} \tag{4}$$

where μ is the viscosity, μ_0 is the permeability of free space and $\bar{\mu}$ is the magnetic susceptibility and

$$g(h)=\left[\frac{1+4s}{1+2s}\right]\left[\left(h+p_a p'\delta\right)^3\sin^3\omega+\left(3\sigma^2+4\alpha^2\right)\left(h+p_a p'\delta\right)\sin\omega\right.$$
$$\left.+3\alpha\left(h+p_a p'\delta\right)^2\sin^2\omega+4\sigma^2\alpha+\alpha^3+\varepsilon\right]+12\phi H_0 \tag{5}$$

where, p' is the reference pressure as in Prajapati [24]. The associated boundary conditions are

$$p\left(a\cos ec\omega\right)=0 \text{ and } p\left(b\cos ec\omega\right)=0 \tag{6}$$

Solving the above Eq. (4) under the boundary conditions (6), one can have,

$$p=0.5\mu_0\bar{\mu}K\left(a\cos ec\omega-x\right)\left(x-b\cos ec\omega\right)$$
$$+\frac{3\mu\dot{h}\sin\omega}{g(h)}\left[\left(x^2-a^2\cos ec^2\omega\right)+\frac{\left(a^2-b^2\right)\cos ec^2\omega}{\ln\left(b/a\right)}\ln\left(\frac{x\sin\omega}{a}\right)\right] \tag{7}$$

Also, the load carrying capacity

$$w=2\pi\int_{b\cos ec\omega}^{a\cos ec\omega}xp\,dx \tag{8}$$

takes the form

$$w=\pi\left(a^2-b^2\right)^2\left[\frac{\mu_0\bar{\mu}K}{12}\left(\frac{a-b}{a+b}\right)-\frac{3\mu\dot{h}\sin\omega}{2g(h)}\left(\frac{a^2+b^2}{a^2-b^2}+\frac{1}{\ln\left(b/a\right)}\right)\right]\cos ec^4\omega. \tag{9}$$

In view of non-dimensional quantities;

$$X=\frac{x}{a},\ \lambda=\frac{b}{a},\ \bar{\sigma}=\frac{\sigma}{h_0},\ \bar{\alpha}=\frac{\alpha}{h_0},\ \bar{\varepsilon}=\frac{\varepsilon}{h_0^3},\ \bar{\delta}=\frac{\delta}{h},\ \bar{p}=p_a p',\ \psi=\frac{\phi H_0}{h_0^3},\ \mu^*=-\frac{h_0^3\mu_0\bar{\mu}K}{\mu\dot{h}}$$

$$P=-\frac{h_0^3\sin\omega}{\mu\dot{h}\pi\left(a^2-b^2\right)}p,\quad W=-\frac{h_0^3\sin^2\omega}{\mu\dot{h}\pi^2\left(a^2-b^2\right)^2}w$$

and

$$G(h)=\frac{g(h)}{h_0^3}=\left[\frac{1+4s}{1+2s}\right]\left[\left(1+\bar{p}\bar{\delta}\right)^3\sin^3\omega+\left(3\bar{\sigma}^2+4\bar{\alpha}^2\right)\left(1+\bar{p}\bar{\delta}\right)\sin\omega\right.$$
$$\left.+3\bar{\alpha}\left(1+\bar{p}\bar{\delta}\right)^2\sin^2\omega+4\bar{\sigma}^2\bar{\alpha}+\bar{\alpha}^3+\bar{\varepsilon}\right]+12\psi \tag{10}$$

One obtains the expressions for non-dimensional pressure distribution and load carrying capacity as follows:

$$P=\frac{\mu^*\left(1-X\sin\omega\right)\left(X-\lambda\cos ec\omega\right)}{2\pi\left(1-\lambda^2\right)}+\frac{3\left(1-X^2\sin^2\omega\right)}{\pi G(h)\left(1-\lambda^2\right)}-\frac{3\ln\left(X\sin\omega\right)}{\pi G(h)\ln(\lambda)}; \tag{11}$$

$$W=\frac{\mu^*\cos ec^2\omega}{12\pi}\left(\frac{1-\lambda}{1+\lambda}\right)+\frac{3\cos ec\omega}{2\pi G(h)}\left[\frac{1+\lambda^2}{1-\lambda^2}-\frac{1}{\ln\lambda}\right]. \tag{12}$$

3. RESULTS AND DISCUSSION

It is clearly seen that the load distribution in the bearing is determined from the Eq. (12). It is revealed that the load carrying capacity increases by

$$\frac{\mu^*}{12\pi}\left[\frac{1-\lambda}{1+\lambda}\right]\cos ec^2\omega$$

as compared to that of a system dealing with the conventional lubricants. It is easy to see that the expression found in Eq. (12) is linear with respect to the magnetization parameter μ^* and hence, increasing values of μ^* would result in increased load carrying capacity. The load carrying capacity registers a sharp rise. However, the effect of the porosity on the distribution of load carrying capacity with respect to μ^* is nominal as can be seen from Fig. 2.

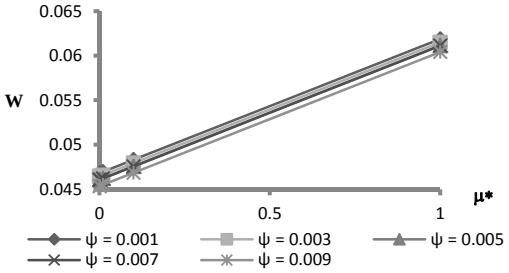

Fig. 2. Variation of Load carrying capacity with respect to μ^* and ψ

The effect of standard deviation on the variation of load carrying capacity is presented in Figs. 3-9. As it is seen, the effect of $\bar{\sigma}$ is quite adverse as it decreases the load carrying capacity. Fig 5 makes it clear that the effect of the porosity on the variation of load carrying capacity with respect to the standard deviation is almost negligible. Further, the effect of bearing deformation on the distribution of load carrying capacity with respect to $\bar{\sigma}$ is, moreover, less negligible which is indicated by Fig. 9.

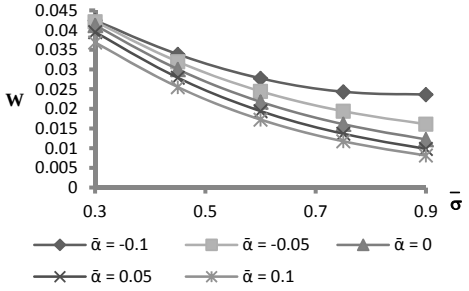

Fig. 3. Variation of Load carrying capacity with respect to $\bar{\sigma}$ and $\bar{\alpha}$

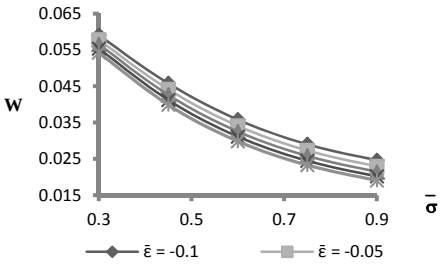

Fig. 4. Variation of Load carrying capacity with respect to $\bar{\sigma}$ and $\bar{\varepsilon}$

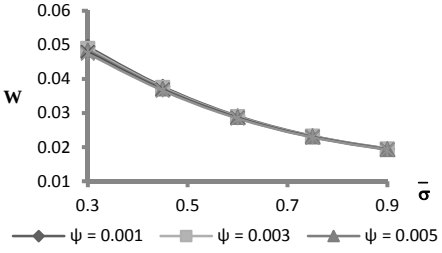

Fig. 5. Variation of Load carrying capacity with respect to $\bar{\sigma}$ and ψ

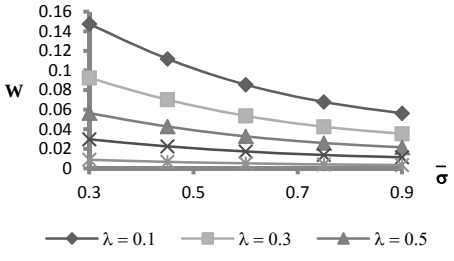

Fig. 6. Variation of Load carrying capacity with respect to $\bar{\sigma}$ and λ

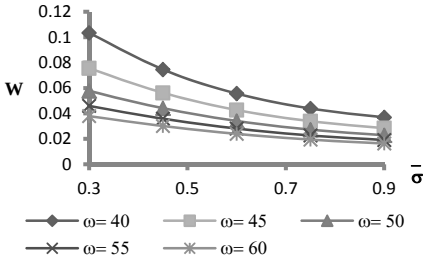

Fig. 7. Variation of Load carrying capacity with respect to $\overline{\sigma}$and ω

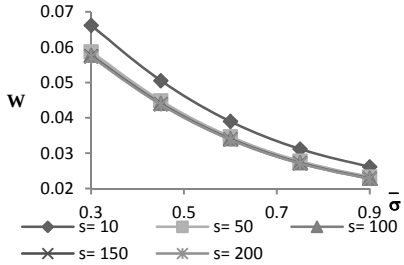

Fig. 8. Variation of Load carrying capacity with respect to $\overline{\sigma}$ and s

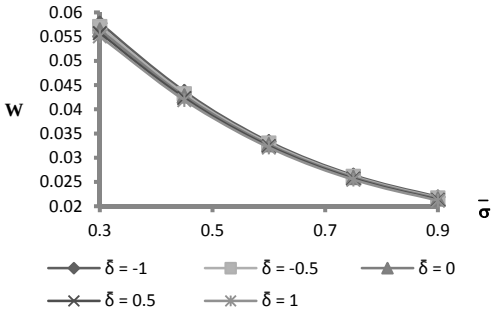

Fig. 9. Variation of Load carrying capacity with respect to $\overline{\sigma}$and $\overline{\delta}$

The fact that positive $\overline{\alpha}$ decreases the load carrying capacity while the load carrying capacity increases due to negative $\overline{\alpha}$ can be noticed from Figs. 10-15. Interestingly, it is found that the effect of the bearing deformation on the distribution of load carrying capacity with respect to $\overline{\alpha}$ is not that significant. Further, the effect of slip velocity on the distribution of load carrying capacity decreases for higher values of the slip parameter, this can be seen from Fig. 14.

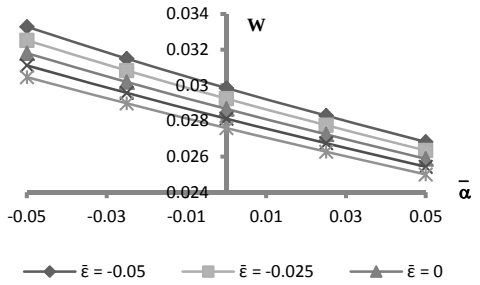

Fig. 10. Variation of Load carrying capacity with respect to $\overline{\alpha}$ and $\overline{\varepsilon}$

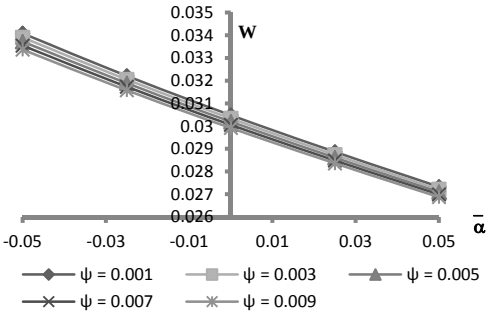

Fig. 11. Variation of Load carrying capacity with respect to $\overline{\alpha}$ and ψ

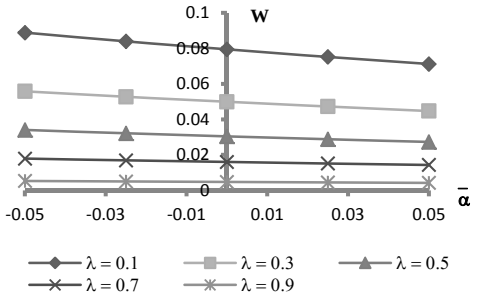

Fig. 12. Variation of Load carrying capacity with respect to $\overline{\alpha}$ and λ

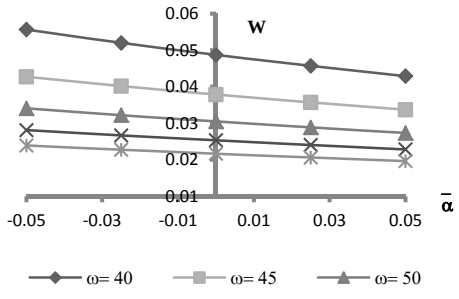

Fig. 13. Variation of Load carrying capacity with respect to $\overline{\alpha}$ and ω

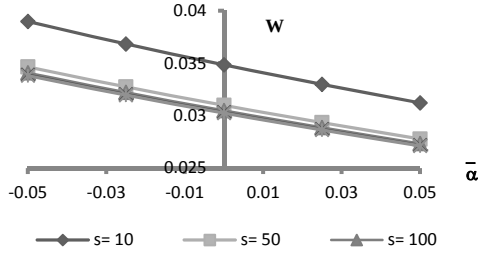

Fig. 14. Variation of Load carrying capacity with respect to $\bar{\alpha}$ and s

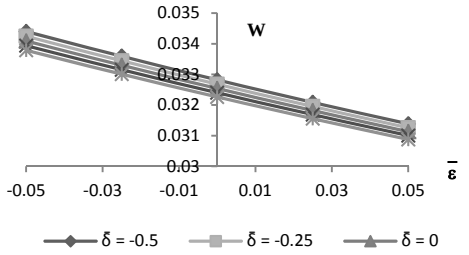

Fig. 15. Variation of Load carrying capacity with respect to $\bar{\alpha}$ and $\bar{\delta}$

One can easily observe that the effect of the skewness is almost identical to the trends of $\bar{\alpha}$ so far as load distribution is concerned (Figs. 16-20). However, here the effect of the deformation $\bar{\delta}$ is quite significant unlike in the case of $\bar{\alpha}$.

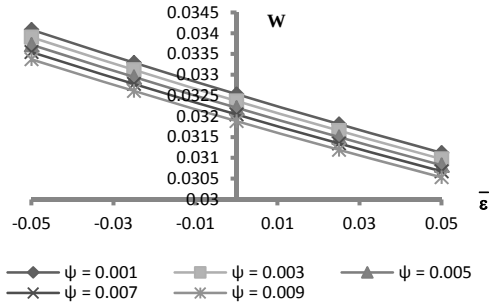

Fig. 16. Variation of Load carrying capacity with respect to $\bar{\varepsilon}$ and ψ

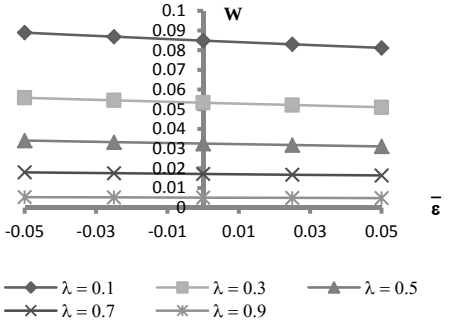

Fig. 17. Variation of Load carrying capacity with respect to $\bar{\varepsilon}$ and λ

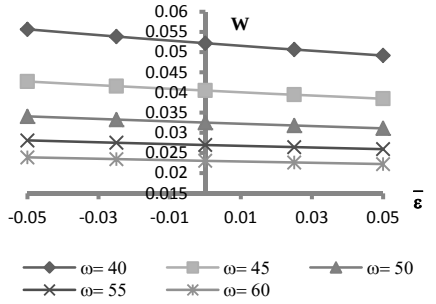

Fig. 18. Variation of Load carrying capacity with respect to $\bar{\varepsilon}$ and ω

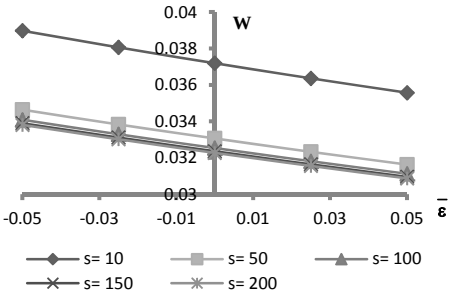

Fig. 19. Variation of Load carrying capacity with respect to $\bar{\varepsilon}$ and s

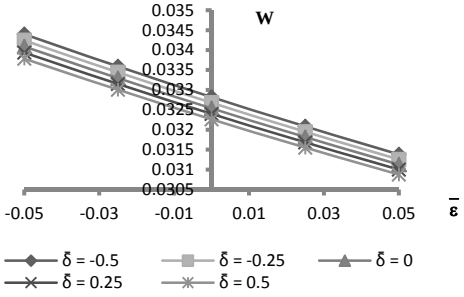

Fig. 20. Variation of Load carrying capacity with respect to $\bar{\varepsilon}$ and $\bar{\delta}$

Increasing values of the porosity parameter cause reduced load carrying capacity as indicated by Figs. 21-24. It is appealing to note that this effect on load carrying capacity is relatively less in the case of aspect ratio λ. On the other hand, the combined effect of porosity and slip velocity and, porosity and

deformation is significant. The effect of aspect ratio presented in Figs. 25-26 makes it clear that the load carry capacity decreases significantly with the increase in aspect ratio. Further, the effect of slip velocity on the distribution of load carrying capacity with respect to aspect ratio is not that significant for relatively higher values of slip parameter which in fact, is a good sign to be noticed. Identically, the effect of slip velocity on the variation of load carrying capacity with respect to the semi-vertical angle is also not that significant for higher values of slip parameter, which is suggested from Fig. 27. Lastly, Fig. 28 bears the stamp of the significantly adverse effect of the combination of slip and deformation.

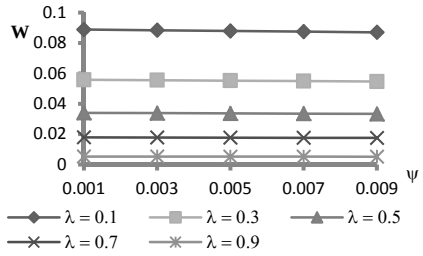

Fig. 21. Variation of Load carrying capacity with respect to ψ and λ

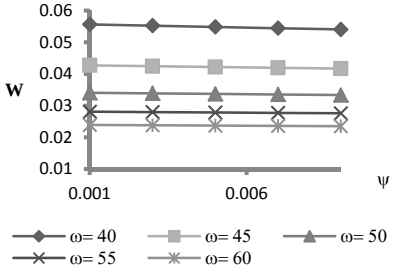

Fig. 22. Variation of Load carrying capacity with respect to ψ and ω

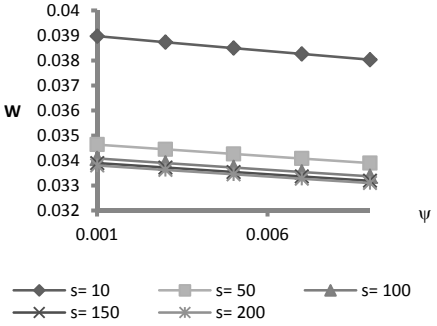

Fig. 23. Variation of Load carrying capacity with respect to ψ and s

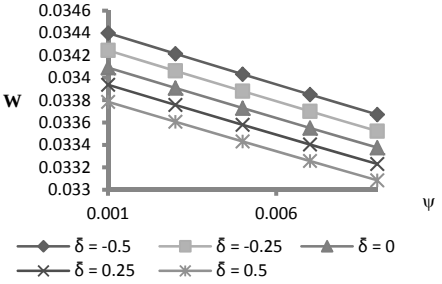

Fig. 24. Variation of Load carrying capacity with respect to ψ and $\bar{\delta}$

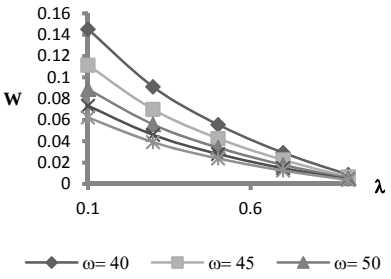

Fig. 25. Variation of Load carrying capacity with respect to λ and ω

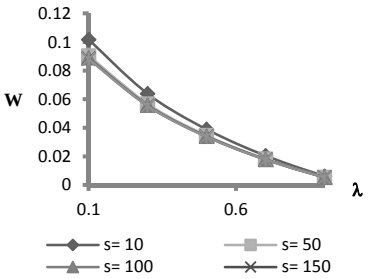

Fig. 26. Variation of Load carrying capacity with respect to λ and s

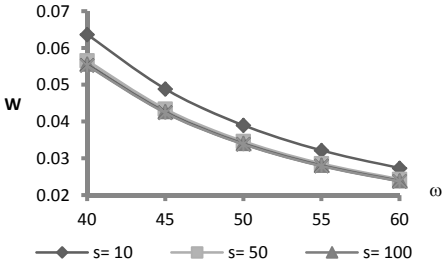

Fig. 27. Variation of Load carrying capacity with respect to ω and s

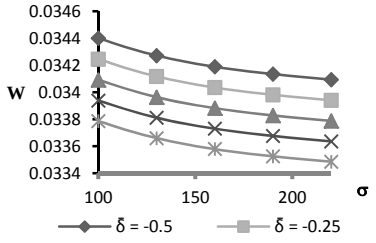

Fig. 28. Variation of Load carrying capacity with respect to s and $\bar{\delta}$

Some of the Figures reveal that the negative effect induced by porosity and deformation can be neutralized by the positive effect of magnetization, at least in the case of negatively skewed roughness for relatively higher values of semi-vertical angle. In the present investigation, it is quite clear that the magnetization has a very limited scope of compensating the entire adverse effect of transverse surface roughness. However, it can go a long way in minimizing this adverse effect for a large range of deformation when relatively higher values of slip parameter are involved.

4. VALIDATION

		Load carrying capacity in this manuscript		**Deheri et al [6]**
Quantity		With consideration	Without consideration	Without consideration
$\bar{\varepsilon} = -0.05$	μ^*	0.042157	0.042144	5.94248
	$\bar{\alpha}$	0.033284	0.032777	4.61504
	$\bar{\sigma}$	0.057765	0.056258	5.949326
	$\bar{\delta}$	0.0344	0.033893	-----
	ψ	0.034085	0.032578	4.992667
	λ	15.26915	-----	
	ω	0.088923	-----	19.65482

		Load carrying capacity in this manuscript		**Deheri et al [6]**
Quantity		With consideration	Without consideration	Without consideration
$\bar{\alpha}$ = **-0.05**	μ^*	0.046815	0.046813	4.61382
	$\bar{\delta}$	0.0344	0.032893	----
	$\bar{\sigma}$	0.042484	0.042371	4.75558
	$\bar{\varepsilon}$	0.033284	0.031777	4.615104
	ψ	0.034085	0.032578	4.919065
	λ	0.473507	0.473204	4.893012
	ω	0.055663	0.048728	5.842398

		Load carrying capacity in this manuscript		**Deheri et al [6]**
Quantity		With consideration	Without consideration	Without consideration
ψ = **0.001**	μ^*	0.046815	0.046813	4.919078
	$\bar{\alpha}$	0.033064	0.033057	4.919034
	$\bar{\varepsilon}$	0.034181	0.032456	4.834085
	$\bar{\delta}$	0.0344	0.034493	---
	$\bar{\sigma}$	0.049473	0.049744	5.063544
	λ	0.034085	---	3.02872
	ω	0.088923	---	9.433781

		Load carrying capacity in this manuscript		**Deheri et al [6]**
Quantity		With consideration	Without consideration	Without consideration
λ = **0.6**	μ^*	0.046815	0.046813	4.919078
	$\bar{\alpha}$	0.033064	0.033057	4.919034
	$\bar{\varepsilon}$	0.034181	0.032456	4.834085
	$\bar{\delta}$	0.0344	0.034493	---
	$\bar{\sigma}$	0.049473	0.049744	5.063544
	ω	0.041606	---	5.753809

		Load carrying capacity in this manuscript		**Deheri et al [6]**
Quantity		With consideration	Without consideration	Without consideration
$\omega = 50$	μ^*	0.046815	0.046813	4.919078
	$\bar{\alpha}$	0.033064	0.033057	4.919034
	$\bar{\varepsilon}$	0.034181	0.032456	4.834085
	$\bar{\delta}$	0.0344	0.034493	---
	$\bar{\sigma}$	0.049473	0.049744	5.063544
	λ	0.038977	---	3.028725

A close scrutiny of the results presented here in comparison with the above investigation suggest that deformation induced adverse effect is not that sharp.

The roughness and deformation obstruct the fluid flow, as a result less pressure is generated but at the same time the magnetization increases the effective viscosity of the lubricant. This effect is further enhanced by the negatively skewed roughness. Consequently, in this situation the combined positive effect of magnetization and negatively skewed roughness does not allow the pressure to fall rapidly.

5. CONCLUSION

This investigation strongly suggests that the roughness aspects must be accorded priority while designing the bearing system. For an overall effective performance of the bearing, the slip parameter is required to be minimized. Further, the values of the slip must be minimized for at least higher values of the deformation. Probably, the enhanced viscosity due to magnetization prevents the load carrying capacity to decrease even if higher value of slip parameter is involved. Of course, in these types of systems there is a limited effect of magnetization in the case of negatively skewed roughness even when negative variance is involved as load carrying capacity reduces greatly owing to the adverse effect of standard deviation, porosity, deformation and slip velocity.

Acknowledgement: The authors acknowledge with thanks the fruitful and pointed comments and suggestions of the reviewers and the editor.

NOMENCLATURE

h	fluid film thickness at any point	$\bar{h}$	the mean film thickness
h_S	deviation from the mean film thickness	ψ	porosity in non-dimensional form
p	lubricant pressure	P	dimensionless pressure
w	load carrying capacity	W	dimensionless load carrying capacity
α	variance	$\bar{\alpha}$	variance in non-dimensional form
σ	standard deviation	$\bar{\sigma}$	dimensionless standard deviation
ε	Skewness	$\bar{\varepsilon}$	non-dimensional skewness
μ	viscosity of lubricant	μ^*	dimensionless magnetization parameter
δ	deformation	$\bar{\delta}$	dimensionless deformation
p_a	the reference ambient pressure	s	slip velocity parameter
$a,\ b$	radius of the lower and upper plates	ω	the inclination angle of magnetic field with the lower plate

REFERENCES

1. Prakash, J. & Vij, S. K. (1973). Load capacity and time height relation between porous plates. *Wear*, Vol. 24, pp. 309-322.
2. Verma, P. D. S. (1986). Magnetic fluid-based squeeze film. *International Journal of Engineering Science*, Vol. 24, No. 3, pp. 305-401.
3. Bhat, M. V. & Deheri, G. M. (1991). Squeeze film behavior in porous annular disks lubricated with magnetic fluid. *Wear*, Vol.151, pp. 123-128.

4. Bhat, M. V. & Deheri, G. M. (1992). Magnetic fluid based squeeze film between two curved circular plates. *Bulletin of Calcutta Mathematical Society,* Vol. 85, pp. 521-524.
5. Hsiu , Chiang, Lu., Cheng, Hsu, H. & Lin, J. R. (2004), Lubrication performance of long journal bearings considering effects of couple stresses and surface roughness. *Journal of the Chinese Institute of Engineers*, Vol. 27, No. 2, pp. 287-292.
6. Deheri, G. M., Patel, H. C. & Patel, R. M. (2007). Magnetic fluid-based squeeze film between rough porous truncated conical plates. *Journal of Engineering Tribology,* Vol. 221, Part J, pp. 515- 523.
7. Christensen, H. & Tonder, K. C. (1969a). Tribology of rough surfaces: stochastic models of hydrodynamic lubrication. *SINTEF Report* No.10/69-18.
8. Christensen, H. & Tonder, K. C. (1969b). Tribology of rough surfaces: parametric study and comparison of lubrication model. *SINTEF Report* No.22/69-18.
9. Christensen, H. & Tonder, K. C. (1970). The hydrodynamic lubrication of rough bearing surfaces of finite width. *ASME-ASLE Lubrication Conference, Paper no.70-lub-7.*
10. Gupta, J. L. & Deheri, G. M. (1996), Effect of roughness on the behavior of squeeze film in a spherical bearing. *Tribology Transaction,* Vol. 39, pp. 99-102.
11. Andharia, P. I., Gupta, J. L. & Deheri, G. M. (2001), Effects of surface roughness and hydrodynamic lubrications of slider bearings, *Tribology Transaction,* Vol. 44, No. 2, pp. 291-297.
12. Hsu, C.H., Lu, R. F. & Lin, J. R. (2009). Combined effects of surface roughness and rotating inertia on the squeeze film characteristics of parallel circular disks. *Journal of Marine Science and Technology,* Vol. 7, No.1, pp. 60-66.
13. Schwarz, U. B. (2003). A generalized analytical model for the elastic deformation of an adhesive contact between a sphere and a flat surface. *Journal of Colloid and Interface Science,* Vol. 261, No. 1, pp. 99-106.
14. Shimpi, M. E. & Deheri, G. M. (2012a). Magnetic fluid-based squeeze film performance in rotating curved porous circular plates: the effect of deformation and surface roughness. *Tribology in Industry,* Vol. 34, No. 2, pp. 57-67.
15. Shimpi, M. E. & Deheri, G. M. (2012b). A study on the performance of a magnetic fluid-based squeeze film in curved porous rotating rough annular plates and deformation effect. *Tribology International,* Vol. 47, pp. 90-99.
16. Shimpi, M. E. & Deheri, G. M. (2013). Surface roughness effect on a magnetic fluid-based squeeze film between a curved porous circular plate and a flat circular plate. *Journal of the Brazilian Society of Mechanical Sciences and Engineering,* (Online).
17. Shah, R. C. & Patel, N. I. (2012). Mathematical modeling of slider bearing of various shapes with combined effects of porosity at both the ends, anisotropic permeability, slip velocity, and squeeze velocity. *American Journal of Computational and Applied Mathematics,* Vol. 2, No.3, pp. 94-100.
18. Mirea, M. & Voicu, C. O. (2012). Study regarding the bearing capacity of truncated cone and hemispherical foundations realized in punched holes. *SGEM2012 Conference Proceedings* (*June 17-23*), No. 2, pp. 275-282.
19. Sameh E. Ahmed & Mahdy, A. (2012). Natural convection flow and heat transfer enhancement of a nanofluid past a truncated cone with magnetic field effect. *World Journal of Mechanics,* Vol. 2, No.5, pp. 272-279.
20. Nassab, S. A. G., Sohi, H. & Zaim, E. H. (2011). Study of lubricant compressibility effect on hydrodynamic characteristics of heavily loaded journal bearings. *Iranian Journal of Science and Technology-Transactions of Mechanical Engineering*, Vol. 35, No.M1, pp. 101-105.
21. Rahmatabadi, A. D. & Rashidi, R. (2006). Effect of mount angle on static and dynamic characteristics of gas-lubricated, noncircular journal bearings. *Iranian Journal of Science and Technology Transaction-B-Engineering*, Vol. 30, No.B3, pp. 327-337.

22. Nassab, S. A. G. & Moayeri, M. S. (2000). A Two-dimensional thermohydrodynamic analysis of journal bearings characteristics. *Iranian Journal of Science and Technology Transaction-B-Engineering*, Vol. 24, No.3, pp. 203-220.
23. Tzeng, S. T. & Saibel, E. (1967).Surface roughness effect on slider bearing lubrication. *ASLE Transaction*, Vol.10, pp. 334-338.
24. Prajapati, B. L. (1995). On certain theoretical studies in hydrodynamic and electromagneto hydrodynamic lubrication. *Ph.D. Thesis Sardar Patel University*. Vallabh Vidyanagar, Anand, Gujarat, India.